Definitions/symmetry-logo-eps-converted-to.pdf

MDPI

Article

Results and perspectives from the first two years of neutrino physics at the LHC by the SND@LHC experiment

The SND@LHC Collaboration[†]

† The names of the members of the SND@LHC Collaboration are provided at the back of the article
* Correspondence: Eric.van.Herwijnen@cern.ch, Giovanni.de.Lellis@cern.ch

Abstract: After a rapid approval and installation, the SND@LHC Collaboration was able to take data successfully in 2022 and 2023. Neutrino interactions from ν_μs originating at the LHC IP1 were observed. Since muons constitute the major background for neutrino interactions, the muon flux entering the acceptance was also measured. To improve the rejection power of the detector and to increase the fiducial volume a third Veto plane was recently installed. The energy resolution of the calorimeter system was measured in a test beam. This will help with the identification of ν_e interactions that can be used to probe charm production in the pseudo-rapidity range of SND@LHC ($7.2 < \eta < 8.4$). Muon trident events have also been observed in the target. To enhance SND@LHC's physics case an upgrade is planned for HL-LHC that will increase the statistics and reduce the systematics. The installation of a magnet will allow the separation of ν_μ from $\overline{\nu}_\mu$.

Keywords: SND@LHC; neutrino; neutrino interactions; electron neutrino; muon neutrino; tau neutrino; flavour violation

1. Introduction

It has been known for some time that pp colliders such as the LHC provide a copious source of multi TeV 'prompt' neutrinos produced at the pp intersections [1]. The scattering of these intense, highly energetic, neutrino beams paves the way to an interesting physics program [2]. In addition, the high muon flux, which is a background for the neutrino physics, allows the study of μp and μN interactions such as the production of muon tridents [3]. To profit from the fact that the flavour composition and energy range of the neutrino flux depend on the pseudorapidity η, the SND@LHC detector was placed in the TI18 tunnel at a distance of 480 m from IP 1 (ATLAS), where it is shielded by about hundred meters of rock. The detector was placed slightly off the LHC beam axis and covers the η range $7.2 < \eta < 8.4$, which is inaccessible by the other experiments at the LHC [4]. It allows the identification of all three flavours of neutrino interactions with high efficiency.

Using the data taken in 2022, 8 events consistent with ν_μ charged-current (CC) interactions were observed, while the estimated background of 0.086 events yielded a significance of about 7 standard deviations [5]. Also using 2022 data, the FASER Collaboration [6] reported the observation of neutrino interactions in a complementary pseudo-rapidity region ($\eta > 8.8$). The muon flux was independently measured by SND@LHC using three different subsystems, each giving compatible results [7]. In this article we shall review and update the results that were obtained during the first two years of data taking, and discuss how this experience led to various improvements of the detector. We shall also give the perspectives for an upgrade that is planned for the high-luminosity LHC phase (HL-LHC).

2. Detector

Figure 1 shows the SND@LHC detector. It is a hybrid detector consisting of emulsion and electronic detectors. The electronic detectors provide the time stamp of the neutrino

CERN-OPEN-2024-003
29/02/2024

check for updates

Citation: . *Symmetry* **2024**, *1*, 0.

Received:
Revised:
Accepted:
Published:

interaction, preselect the interaction region while the neutrino interaction vertex is reconstructed using tracks in the emulsion. The Veto system is used to tag muons and other charged particles entering the detector from the IP1 direction.

The Veto system consists of two parallel planes of scintillating bars. Each plane is made of seven $1 \times 6 \times 42$ cm^3 vertically stacked bars of plastic scintillator.

The target section contains five walls. Each wall consists of four units ('bricks') of Emulsion Cloud Chambers (ECC) and is followed by a scintillating fiber (SciFi) station for tracking.

Each SciFi station consists of one horizontal and one vertical 39×39 cm^2 plane. Each plane comprises six staggered layers of 250 µm diameter polystyrene-based scintillating fibers. The single particle spatial resolution in one plane is ∼100 µm and the time resolution for a particle crossing both x and y planes is about 250 ps.

The muon system consists of two parts: the first five stations (UpStream, US), and the last three stations (Down Stream (DS), see Figure 1). Each US station consists of 10 stacked horizontal scintillator bars of $82.5 \times 6 \times 1$ cm^3, resulting in a coarse y view. A DS station consists of two layers of thinner bars measuring $82.5 \times 1 \times 1$ cm^3, arranged in alternating x and y planes, allowing for a spatial resolution in each axis of less than 1 cm. The eight scintillator stations are interleaved with 20 cm thick iron blocks. Events with hits in the DS detector and the SciFi tracker are used to identify muons.

All signals exceeding preset thresholds are read out by the front-end electronics and clustered in time to form events. An efficient software noise filter is applied to the events online, resulting in negligible detector deadtime and negligible loss in signal efficiency. Events satisfying certain topological criteria, such as the presence of hits in several detector planes, are read out. At the highest instantaneous luminosity in 2022 (2.5×10^{34} cm^{-2} s^{-1}) this generated a rate of around 5.4 kHz.

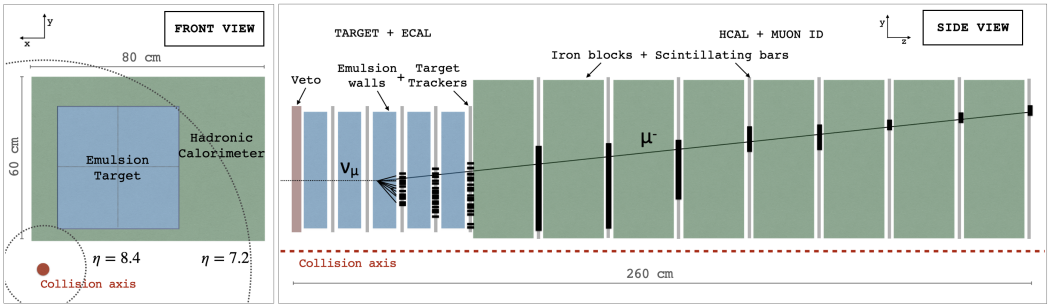

Figure 1. Schematic layout of the SND@LHC detector. The pseudo-rapidity η values are the limits for particles hitting the lower left and the upper right corner of the ECC. The side view includes an illustration of a simulated ν_μ CC interaction.

3. Dataset and simulated samples

During 2022 and 2023 data was taken with pp collisions at a center of mass energy of 13.6 TeV. A total integrated luminosity of 70.5 fb^{-1} (36.8 fb^{-1} in 2022, 33.7 fb^{-1} in 2023) was recorded with an efficiency of 97.3 % (95 % in 2022, 99.7 % in 2023).

The analysis developed for the observation of ν_μ CC interactions from LHC collisions was conducted solely using the data from the electronic detectors. The information from the emulsion detector is currently being processed and will require more time to analyze.

Neutrino production in pp collisions at the LHC is simulated with the FLUKA Monte Carlo simulation program [8]. DPMJET3 (Dual Parton Model, including charm) [9] is used for the pp event generation, and FLUKA performs the particle propagation towards the SND@LHC detector with the help of a detailed simulation of LHC accelerator elements. FLUKA also takes care of simulating the production of neutrinos from decays of long-lived products of the pp collisions and of particles produced in re-interactions with the surrounding material. GENIE [10] is then used to simulate neutrino interactions with the

detector material. The propagation of particles through the TI18 tunnel and the SND@LHC detector is simulated with GEANT4 [11]. A total of around 1.6×10^5 simulated neutrino events and 3×10^7 background events were generated for the analyses described in this publication.

4. Muon neutrino interactions

Given the high energy of the neutrinos within the detector acceptance [4], the dominant charged current (CC) process occurring for ν_μs is deep inelastic scattering (CC DIS). The signature of these interactions includes an isolated muon track in the muon system, associated with a hadronic shower detected in the SciFi and hadronic calorimeter. In Figure 1 the distinctive topology of ν_μ CC DIS interactions is shown.

Considering the mass of the tungsten target during the 2022 run ($\sim$ 800 kg), about 157 $\pm$ 37 ν_μ CC DIS interactions are expected in the full target in the analysed data set. The large range in the expectation is caused by the difference between the predictions of the ν_μ flux at SND@LHC from DPMJET3 and SIBYLL obtained in Ref. [12]. The modeling is complex and the different Monte Carlo programs have associated uncertainties ranging from 10%–200%.

Observing the rare neutrino signal over the prevailing background implies adopting a selection with strong rejection power, designed to yield a clean set of events. As a result of the full selection, 8 ν_μ CC DIS candidates are identified, while 4.2 are expected [5]. The number of data and simulated signal events passing each section of the event selection criteria is given in Table 1.

Table 1. Number of events passing the selection cuts in the data and signal simulation.

	Data	Signal simulation
All	8.4×10^9	157
Fiducial volume	4.9×10^5	11.9
One muon-like track	17	6.1
Large SciFi activity	13	5.1
Large hadronic activity	12	4.7
Low muon system activity	8	4.2

A candidate event is shown in Figure 2.

To estimate the background from penetrating muons, the inefficiency of the Veto system needs to be measured. The overall Veto system inefficiency during the 2022 was 4.5×10^{-4} [13] whereas during 2023 it was 6.6×10^{-6} [14]. This is due to the fact that, for most of the 2022 run the time alignment between the different detector planes was not in place. The efficiency in 2023 is limited by the dead time.

In 2022, the SciFi inefficiency per station was 1.1×10^{-4} making the combined inefficiency of the Veto system and the two most upstream SciFi planes 5.3×10^{-12}. The background induced by muons entering the fiducial volume is therefore negligible.

5. Muon flux measurement

For the calculation of the muon flux, only muons from pp collisions in IP1 are counted. The LHC filling scheme specifies which bunches cross at IP 1. Since the SND@LHC detector is 480 m away from IP 1, there is a phase shift between the filling scheme and the SND@LHC event timestamp. The phase adjustments for both beams are determined by finding the maximum overlap with SND@LHC event rates. The synchronized bunch structure then allows us to identify events associated with collisions at IP 1.

The muon flux is defined as the number of tracks per IP 1 integrated luminosity and unit detector area. The number of tracks is corrected for the tracking efficiency. The muon flux in the SciFi and DS detectors is estimated in an area with uniform tracking efficiency. For the SciFi this is the area with -42 cm $\leq x \leq -11$ cm and 18 cm $\leq y \leq 49$ cm

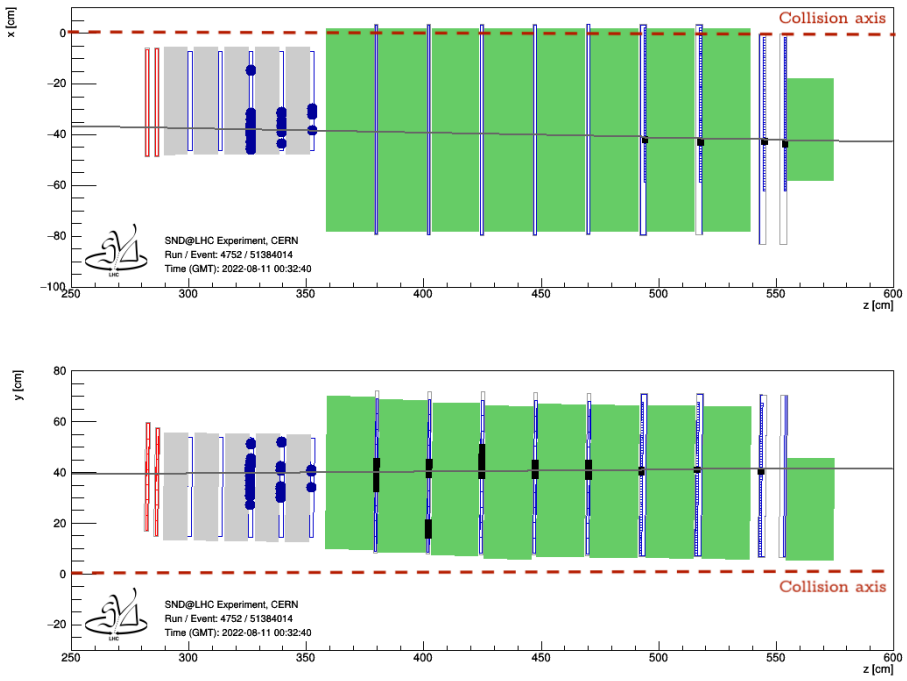

Figure 2. Display of a ν_μ CC candidate event. Hits in the SciFi, and hadronic calorimeter and muon system are shown as blue markers and black bars, respectively, and the line represents the reconstructed muon track. The dotted line in red shows the collision axis.

Table 2. Comparison between the muon flux obtained from data and Monte Carlo simulation.

system	sample	muon flux $[10^4 \text{fb}/\text{cm}^2]$	$1 - \frac{\text{sim}}{\text{data}}$ [%]
SciFi	data	$2.06 \pm 0.01(\text{stat.}) \pm 0.12(\text{sys.})$	22 ± 9
	sim	$1.60 \pm 0.05(\text{stat.}) \pm 0.19(\text{sys.})$	
DS	data	$2.35 \pm 0.01(\text{stat.}) \pm 0.10(\text{sys.})$	24 ± 9
	sim	$1.79 \pm 0.03(\text{stat.}) \pm 0.15(\text{sys.})$	

(31×31 cm^2, see Figure 3 left). For the DS this is the area with -54 cm $\leq x \leq -2$ cm and 12 cm $\leq y \leq 64$ cm (52×52 cm^2, see Figure 3 right) [7].

The muon fluxes per integrated luminosity for SciFi and DS are presented in Table 2, together with the statistical and systematic uncertainties. The DS muon flux is larger than the SciFi flux because of the non-uniform distribution of tracks in the vertical direction and the difference in acceptance. The total relative uncertainty is 6 % for the SciFi measurement and 4 % for the DS.

The flux values obtained from the electronic detectors using data are between 20–25 % larger than those obtained from the Monte Carlo simulation. Given the complexity of modelling and the fact that different Monte Carlo programs are used, each with an associated uncertainty ranging from 10–200 %, the agreement between the prediction by the Monte Carlo simulation and the measured flux is satisfactory.

During the commissioning phase of the LHC (7 May – 26 July 2022), a reduced target was instrumented with a single emulsion brick to establish whether the occupancy of the emulsion could be determined, thus providing input for the analysis of future targets.

The muon flux per integrated luminosity through an 18×18 cm^2 area of this ECC brick was found to be $1.5 \pm 0.1(\text{stat}) \times 10^4$ fb/cm^2, in reasonable agreement with the measurement from the electronic detectors.

Extended measurements of the muon flux are important to validate the FLUKA simulations. A muon telescope has been installed in TI18, during the 2023-2024 YETS. It is

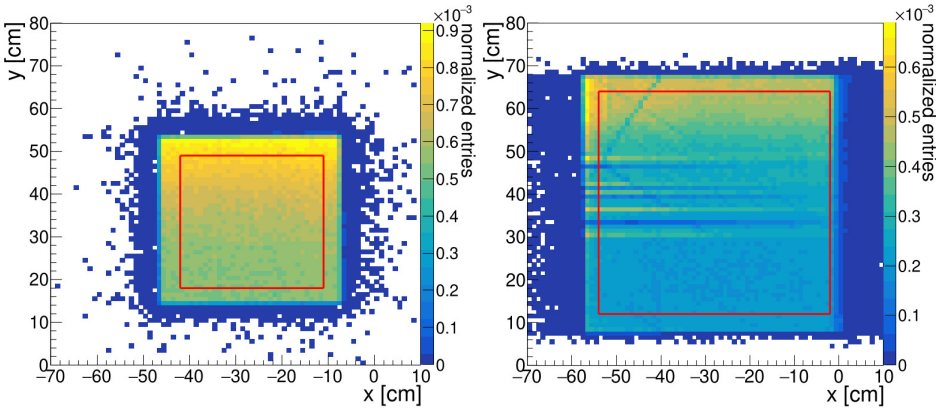

Figure 3. Distribution of SciFi tracks at the most upstream detector plane (left). Distribution of DS tracks at the most upstream detector plane (right). The distributions are normalized to unit integral. Horizontal stripes of lower counts in the central part of the detector are caused by scintillator bar inefficiencies. The red border delimits the region considered for the DS muon flux measurement.

positioned upstream of the SND@LHC target. Its portability should further allow to extend the measurement of the muon flux in different angular regions.

6. Veto upgrade

Table 1 shows that the fiducial volume cut rejects 92.4% of the neutrino CC interactions. This is mostly because of the Veto inefficiency in the bottom part of the detector where the neutrino density is higher. This is shown in Figure 4 where tracks reconstructed with SciFi hits are projected back on the veto planes for events with a low number of fired Veto channels. Besides this reduction of the transverse plane, the use of two SciFi stations to veto non-ν events has further reduced the fiducial volume.

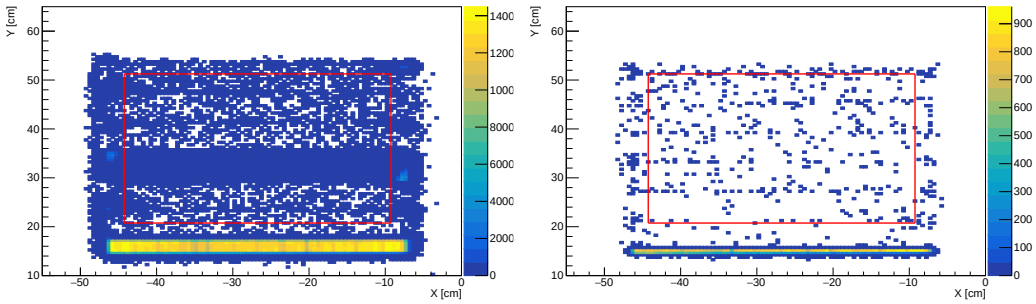

Figure 4. The extrapolated position of the reconstructed Scifi track at Veto plane 0 (left) and Veto plane 1 (right) for events with less than 13 fired Veto channels. The red square encloses the fiducial area used for the observation of neutrino interactions.

To address these issues, a third Veto station with vertical bars was installed during the Year End Technical Stop of 2023–2024 (see Figure 5). The acceptance is increased by the excavation and the shift of the whole Veto system towards the bottom. The new position of the Veto now provides a full coverage of the target sensitive area. Since the lower part of the target has the highest neutrino density, we do expect an increase in the number of observed neutrino interactions although this number has not been evaluated yet. The detector was tested with cosmic rays and is currently being commissioned.

7. Energy calibration

For all neutrino flavours, energetic νN collisions produce electromagnetic and hadronic showers. The reconstruction of the total energy requires an estimate of the fraction lost in

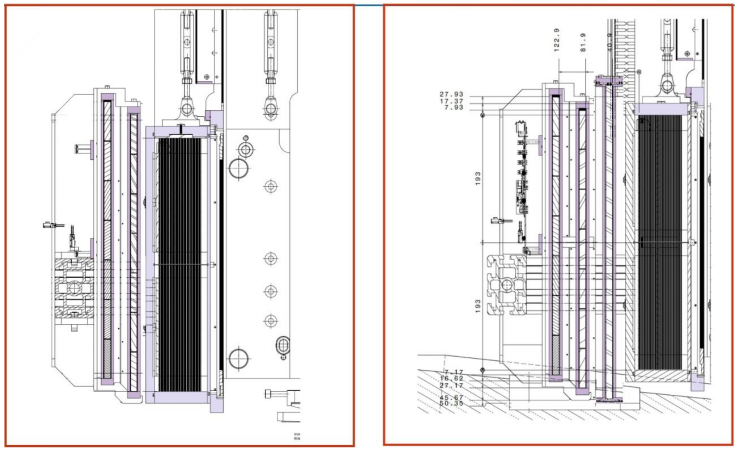

Figure 5. Current Veto system layout with two planes with horizontal bars (left). The upgraded Veto system with a third plane with vertical bars (right).

the target and US regions. The combination of the SciFi + target and Muon system acts as a non-homogeneous hadronic calorimeter with $\approx 11\ \lambda_{\text{int}}$, ranging from 9.5 to 12.5 λ_{int} depending on the position of the neutrino interaction vertex in the target, for the measurement of the energy of the hadronic jet produced in the neutrino interaction. The energy of electromagnetic and hadronic showers is obtained by measuring the shower profile at each SciFi plane. The energy calibration for the SciFi tracker was done with a test beam in 2023. The detector layout of the test beam setup is shown in Figure 6. The configuration of the

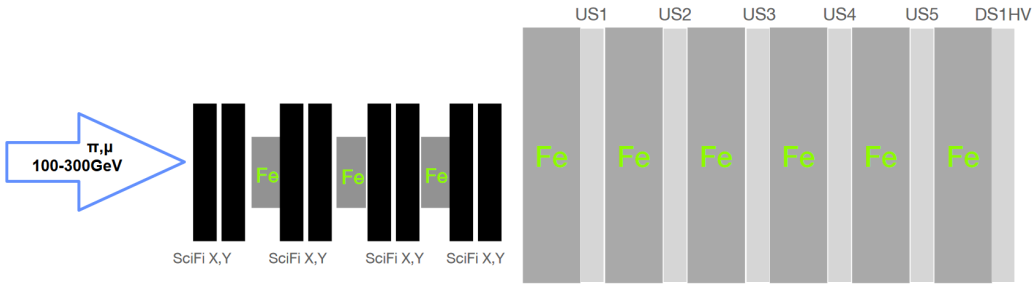

Figure 6. The detector used for the energy calibration.

test beam differs from the setup installed in TI 18 for the following: only one DS station is used and half of the target, equivalent to 1.5 λ_{int} is reproduced with three iron slabs.

The test beam provided pions with energies between 100 and 300 GeV. Figure 7 (left) shows that the energy response of the SciFi is proportional to the energy of the incoming particle, whereas the figure on the right shows that there is a linear correlation between the energy response of the SciFi and the US.

Thus one can assume that the energy may be given as a combination of the QCD[1] values obtained from the two systems:

$$E = k \times QDC_{\text{SciFi}} + \alpha \times QDC_{\text{US}}. \tag{1}$$

By determining the value of the parameters k and α from the measurements one can calculate the reconstructed energy, from which we obtain preliminary figures for the energy resolution of about 25 % at 100 GeV and 15 % at 300 GeV for showers initiated in the second target of the test beam configuration. These preliminary results are shown in Figure 8.

To apply these results to the detector in TI18, one needs to determine the origin of the shower. For showers starting in the last three walls of the target, the results can be applied

[1] QDC (charge-to-digital conversion) is a technique to measure the energy of particles or photons detected by the silicon photomultipliers (SiPMs) that generate signals from the SciFi and the US.

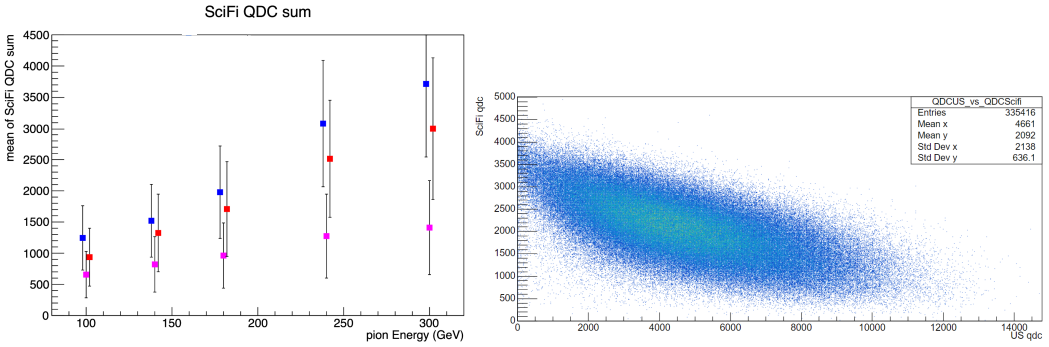

Figure 7. TheSciFi response for particles of various energy. The different colours denote the starting point of the shower (blue indicates wall 1, red 2 and pink 3)(left). The energy response of the SciFi vs the US for 180 GeV pions (right).

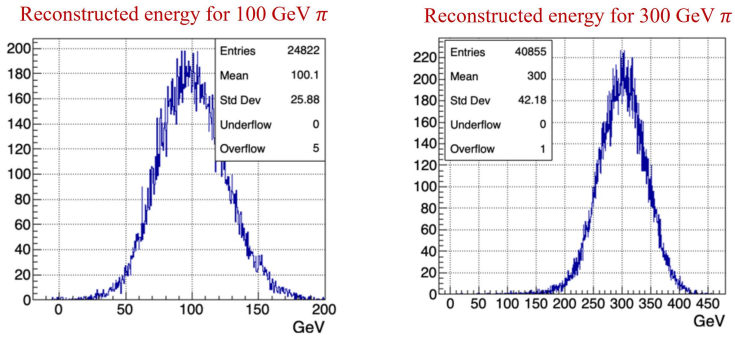

Figure 8. Preliminary results for the reconstructed energy from the 2023 test beam.

without change since the number of interaction lengths is the same. For showers starting in the first two walls, an extrapolation can be done using a Monte Carlo simulation which has been calibrated using the test beam data.

8. Muon trident events

When Pauli postulated the exclusion principle to explain the number of electrons on the shells around the nucleus, muons had not yet been discovered. Since muons behave like electrons in all aspects, states in which two identical muons exist are also antisymmetric to the exchange of these muons [3]. Muon trident events were observed and indeed, the measured cross section conforms to Fermi-Dirac statistics [15]. They were also observed when cosmic muons impinged on the ALEPH RPC detector [16]. However, such events have not yet been observed at the LHC.

In SND@LHC, two types of muon trident-like events have been observed in the 2022 data:

1. Three almost parallel tracks entering the detector (Figure 9, A).
2. An incoming track, a vertex in the target with three outgoing tracks (Figure 9, B).

The events in the first category are muon tridents produced in the upstream rock, whereas the second category are events produced in the detector.

There are two posible sources of these events:

1. $\mu^{\pm} + N \rightarrow \mu^{+}\mu^{-}\mu^{\pm} + N$ (genuine trident).
2. $\mu^{\pm} + N \rightarrow \mu^{\pm} + N + \gamma, \gamma + N \rightarrow N + \mu^{+} + \mu^{-}$ (muon bremsstrahlung followed by gamma conversion).

Note that the cross section for these gamma conversion events was calculated, but not measured [3]. Since these processes were recently introduced in Geant4 [17] our measurement will also be an interesting validation of this implementation. The analysis is in progress.

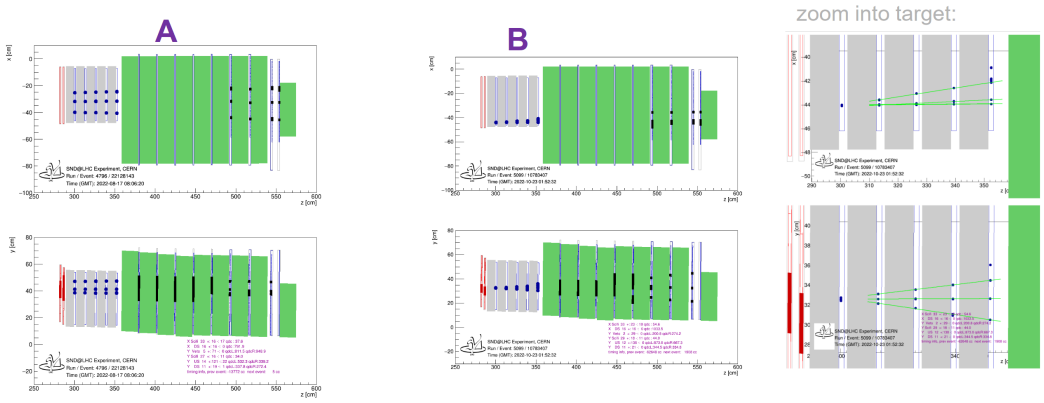

Figure 9. Muon trident-like events detected at SND@LHC.

9. Upgrade plans for the High Luminosity LHC

To improve the detector performance and to overcome the geometrical constraints imposed by the tunnel geometry and the sloping floor, an upgraded version of the detector is proposed for the HL-LHC.

To profit from the high statistics at the HL-LHC and to be able to distinguish neutrinos from anti-neutrinos, two detectors in the forward direction are foreseen: an "AdvSND-Far" detector covering the $\eta > 7.9$ range in TI18 and, in a second stage, an "AdvSND-Near" detector close to IP5 (CMS), covering the $4.0 < \eta < 4.5$ range (see Figure 10). The latter η range overlaps with that of LHCb where $c-$ and $b-$quark production cross sections have been measured. This will allow a significant reduction of the systematic uncertainties in the measurement of heavy quark production in the uprobed forward region that will be conducted with the AdvSND-Far detector.

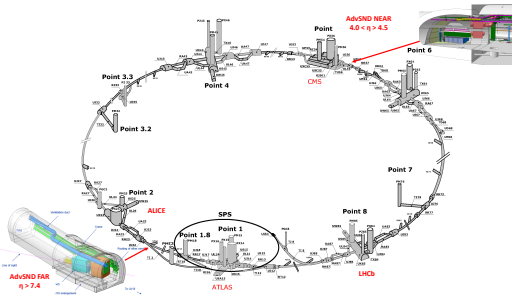

Figure 10. The proposed AdvSND detectors.

The detector structure of AdvSND-Far will closely resemble the current SND@LHC detector, comprising a neutrino target serving as both a vertex detector and an electromagnetic calorimeter (see Figure 11, left). It will be preceded by a charged particle veto setup and followed by a hadron calorimeter and a muon identifier.

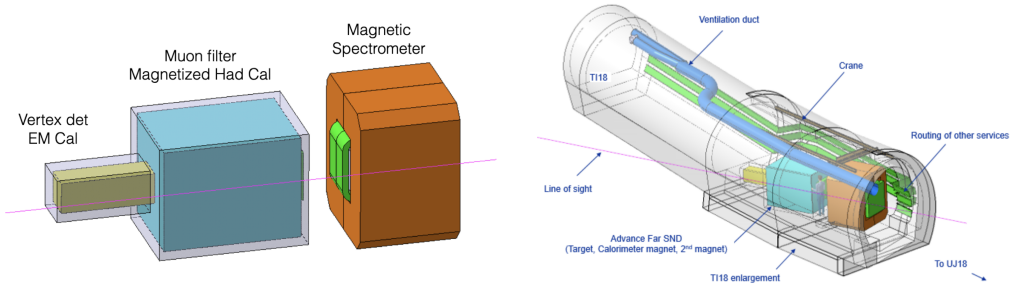

Figure 11. The AdvSND-Far detector (left) and its position in TI18 (right).

During the 2022 and 2023 runs, it was established that the maximum amount of integrated luminosity for the reconstruction of the emulsion data is about 20 fb^{-1}. At this luminosity the pile-up of muons produces parallel tracks $\approx$ 10 micron apart from each other. This is the limit with which consecutive films can be aligned.

At the HL-LHC the expected instantaneous luminosity is five times larger than the current one and the maximum exposure will be obtained after one week. The frequent replacement of emulsion films, even if financially manageable by the Collaboration, would require a correspondingly frequent stop of the machine to provide access, which is not compatible with an efficient operation of the LHC machine. For this reason, the use of an electronically readout technology as a high-precision vertex detector is envisaged. An agreement with CMS was established to re-use their silicon strips tracker stations with a pitch of 122 μm.

The detector is designed to fit within the same area (the TI18 tunnel) with modifications intended to better exploit the neutrino flux (see Figure 11, right). Due to the sloping floor, the veto does not cover the entire target region, and it does not have any rejection power against charged particles entering the lower part of the target, where the neutrino flux is higher. Thus the detector needs to be lowered by 15 cm which means that the base of the tunnel needs to be excavated. At this location there will be a partial overlap with FASER [6] which is useful for comparison and constraints on the systematics. We expect to collect more than 2.5 $\times$ 10^5 ν and $\overline{\nu}$ CC DIS interactions of all flavours (for an integrated luminosity of 3 ab^{-1}), i.e. about hundred times more than what will be collected in Run 3. The ν_e flux in the target is still predominantly (>80%) produced by charmed hadron decays (Figure 12).

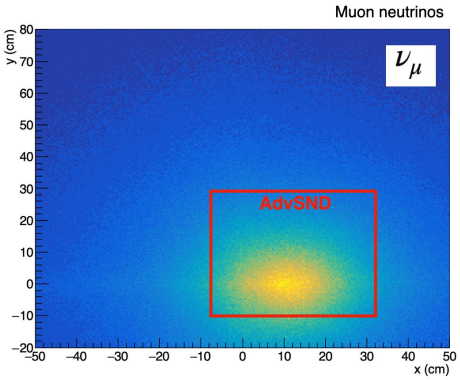

Figure 12. ν_μ flux in the acceptance of the AdvSND-Far target.

A further enhancement is the addition of a magnet to measure the momentum of the muons produced following the neutrino interaction. To allow the installation of a magnet the tunnel section needs to be enlarged.

The AdvSND-Near detector and its position are shown in Figure 13. Preliminary

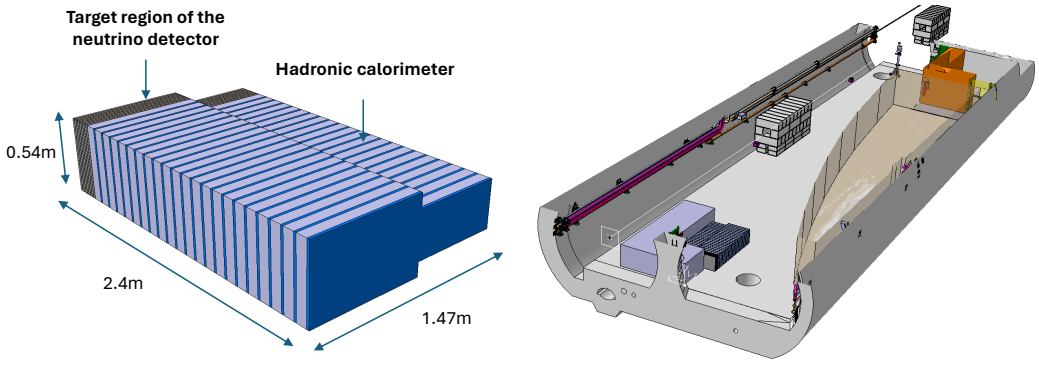

Figure 13. The AdvSND-Near detector (left) and its proposed location in the UJ57 cavern (right).

results of Monte Carlo simulation studies indicate that we can expect 2×10^4 DIS CC neutrino interactions.

10. Conclusions

Using the 2022 data SND@LHC has published the observation of ν_μ interactions at the LHC and the measurement of the μ flux passing through the detector. The operation continued smoothly in 2023 with an improved efficiency of 99.7 %. The analysis of the 2023 data is ongoing and updates will be published soon, including the search for ν_e interactions. The observation of ν_τ interactions requires the processing and analysis of the emulsion data. Interesting muon trident-like events have been detected and a full analysis is underway.

A test beam campaing was conducted in 2023 for the energy calibration. The energy resolution of the electromagnetic and hadronic calorimeters was measured to lie between 15-30 %, as expected from the simulation. To recover fiducial volume losses (bottom part in particular) a third Veto layer was installed and the entire Veto system was lowered during the 2023–2024 YETS.

Studies are in progress on how to extend the physics case during HL-LHC. A Letter of Intent describing the upgrade project is being prepared.

11. Acknowledgements

We express our gratitude to our colleagues in the CERN accelerator departments for the excellent performance of the LHC. We thank the technical and administrative staffs at CERN and at other SND@LHC institutes for their contributions to the success of the SND@LHC effort. We acknowledge and express gratitude to our colleagues in the CERN SY-STI team for the fruitful discussions regarding beam losses during LHC operations. In addition, we acknowledge the support for the construction and operation of the SND@LHC detector provided by the following funding agencies: CERN; the Bulgarian Ministry of Education and Science within the National Roadmap for Research Infrastructures 2020–2027 (object CERN); ANID—Millennium Program—ICN2019_044 (Chile); the Deutsche Forschungsgemeinschaft (DFG, ID 496466340); the Italian National Institute for Nuclear Physics (INFN); JSPS, MEXT, the Global COE program of Nagoya University, the Promotion and Mutual Aid Corporation for Private Schools of Japan for Japan; the National Research Foundation of Korea with grant numbers 2021R1A2C2011003, 2020R1A2C1099546, 2021R1F1A1061717, and 2022R1A2C100505; Fundação para a Ciência e a Tecnologia, FCT (Portugal), CERN/FIS-INS/0028/2021; the Swiss National Science Foundation (SNSF); TENMAK for Turkey (Grant No. 2022TENMAK(CERN) A5.H3.F2-1). M. Climesu, H. Lacker and R. Wanke are funded by the Deutsche Forschungsgemeinschaft (DFG, German Research Foundation), Project 496466340. We acknowledge the funding of individuals by Fundação para a Ciência e a Tecnologia, FCT (Portugal) with grant numbers CEECIND/01334/2018, CEECINST/00032/2021 and PRT/BD/153351/2021. We thank Luis Lopes, Jakob Paul Schmidt and Maik Daniels for their help during the construction.

References

1. A. De Rújula and R. Rückl, Neutrino and muon physics in the collider mode of future accelerators. *In SSC Workshop: Superconducting Super Collider Fixed Target Physics*, **1984**, pp 571—596, https://doi.org/10.5170/CERN-1984-010-V-2.571.
2. N Beni et al., Physics potential of an experiment using LHC neutrinos. *J. Phys. G: Nucl. Part. Phys.*, **2019**, *46*, 115008. DOI 10.1088/1361-6471/ab3f7c
3. M. J. Tannenbaum, Muon Tridents, *Phys. Rev.*, **1968**, *167*, pp 1308–1313.
4. C. Ahdida et al., SND@LHC SND - Scattering and Neutrino Detector at the LHC, *Technical Proposal*, **2021**, CERN-LHCC-2021-003 ; LHCC-P-016.
5. R. Albanese et al. (SND@LHC Collaboration), Observation of Collider Muon Neutrinos with the SND@LHC Experiment. *Phys. Rev. Lett.*, **2023**, *131*, 031802.
6. Henso Abreu et al. (FASER Collaboration), First Direct Observation of Collider Neutrinos with FASER at the LHC, *Phys. Rev. Lett.* **2023**, *131*, 031801.
7. R. Albanese et al. (SND@LHC Collaboration), Measurement of the muon flux at the SND@LHC experiment. *EPJC*, **2024** *84*, 90.
8. G. Battistoni et al., Overview of the FLUKA code, *Ann. Nucl. Energy*, **2015**, *82*, 10.
9. S. Roesler, R. Engel, and J. Ranft, The Monte Carlo Event Generator DPMJET-III. *In Advanced Monte Carlo for Radiation Physics, Particle Transport Simulation and Applications. Proceedings, Conference, MC2000, Lisbon, Portugal*, **2000**, p 1033, arXiv:hep-ph/0012252.
10. C. Andreopoulos et al., The GENIE neutrino Monte Carlo generator, *Nucl. Instrum. Methods Phys. Res.*, **2010**, *Sect. A 614*, 87.
11. S. Agostinelli et al., GEANT4–a simulation toolkit, *Nucl. Instrum. Meth. A*, **2003**, *506*, pp 250–303, SLAC-PUB-9350, FERMILAB-PUB-03-339, CERN-IT-2002-003, DOI 10.1016/S0168-9002(03)01368-8.
12. F. Kling and L. J. Nevay, Forward neutrino fluxes at the LHC, *Phys. Rev. D*, **2021**, *104*, 113008.
13. T. Ruf, Estimate of the Veto System Inefficiency 2022, **2023**, SNDLHC-INT-2023-002.
14. T. Ruf, Estimate of the Veto System Inefficiency 2023, **2023**, SNDLHC-INT-2023-008.
15. J. J. Russel et al., Observation of Muon Trident Production in Lead and the Statistics of the Muon, *Phys. Rev. Lett.*, **1971**, *26*, pp 46–50.
16. F. Maciuc et al., Muon-pair production by atmospheric muons in CosmoALEPH, *Phys. Rev. Lett.*, **2006**, *96(2)*, 021801.
17. S. Yajaman and V. Ivantchenko, The Implementation of $\mu^+\mu^-$ Production by Muons in Geant4, **2022**, CERN-STUDENTS-Note-2022-008.
18. D. Abbaneo et al., AdvSND@LHC- The Advanced Scattering and Neutrino Detector at the LHC, *Letter of Intent*, **2024**, To be submitted to the LHCC, CERN-LHCC-2024-xx.

The SND@LHC Collaboration

D. Abbaneo[9], S. Ahmad[42], R. Albanese[1,2], A. Alexandrov[1], F. Alicante[1,2], K. Androsov[6], A. Anokhina[3], T. Asada[1,2], C. Asawatangtrakuldee[38], M.A. Ayala Torres[32], C. Battilana[4,5], A. Bay[6], A. Bertocco[1,2], C. Betancourt[7], D. Bick[8], R. Biswas[9], A. Blanco Castro[10], V. Boccia[1,2], M. Bogomilov[11], D. Bonacorsi[4,5], W.M. Bonivento[12], P. Bordalo[10], A. Boyarsky[13,14], S. Buontempo[1], M. Campanelli[15], T. Camporesi[9], V. Canale[1,2], A. Castro[4,5], D. Centanni[1,16], F. Cerutti[9], M. Chernyavskiy[3], K.-Y. Choi[17], S. Cholak[6], F. Cindolo[4], M. Climescu[18], A.P. Conaboy[19], G.M. Dallavalle[4], D. Davino[1,20], P.T. de Bryas[6], G. De Lellis[1,2], M. De Magistris[1,16], A. De Roeck[9], A. De Rújula[9], M. De Serio[21,22], D. De Simone[7], A. Di Crescenzo[1,2], D. Di Ferdinando[4], R. Donà[4,5], O. Durhan[23], F. Fabbri[4], F. Fedotovs[15], M. Ferrillo[7], M. Ferro-Luzzi[9], R.A. Fini[21], A. Fiorillo[1,2], R. Fresa[1,24], W. Funk[9], F.M. Garay Walls[25], A. Golovatiuk[1,2], A. Golutvin[26], E. Graverini[6,41], A.M. Guler[23], V. Guliaeva[3], G.J. Haefeli[6], C. Hagner[8], J.C. Helo Herrera[27,40], E. van Herwijnen[26], P. Iengo[1], S. Ilieva[1,2,11], A. Infantino[9], A. Iuliano[1,2], R. Jacobsson[9], C. Kamiscioglu[23,28], A.M. Kauniskangas[6], E. Khalikov[3], S.H. Kim[29], Y.G. Kim[30], G. Klioutchnikov[9], M. Komatsu[31], N. Konovalova[3], S. Kuleshov[27,32], L.Krzempek[1,11], H.M. Lacker[19], O. Lantwin[1], F. Lasagni Manghi[4], A. Lauria[1,2], K.Y. Lee[29], K.S. Lee[33], S. Lo Meo[4], V.P. Loschiavo[1,20], S. Marcellini[4], A. Margiotta[4,5], A. Mascellani[6], F. Mei[5], A. Miano[1,2], A. Mikulenko[13], M.C. Montesi[1,2], F.L. Navarria[4,5], W. Nuntiyakul[39], S. Ogawa[34], N. Okateva[3], M. Ovchynnikov[13], G. Paggi[4,5], B.D. Park[29], A. Pastore[21], A. Perrotta[4], D. Podgrudkov[3], N. Polukhina[3], A. Prota[1,2], A. Quercia[1,2], S. Ramos[10], A. Reghunath[19], T. Roganova[3], F. Ronchetti[6], T. Rovelli[4,5], O. Ruchayskiy[35], T. Ruf[9], M. Sabate Gilarte[9], Z. Sadykov[1], M. Samoilov[3], V. Scalera[1,16], W. Schmidt-Parzefall[8], O. Schneider[6], G. Sekhniaidze[1], N. Serra[7], M. Shaposhnikov[6], V. Shevchenko[3], T. Shchedrina[3], L. Shchutska[6], H. Shibuya[34,36], S. Simone[21,22], G.P. Siroli[4,5], G. Sirri[4], G. Soares[10], J.Y. Sohn[29], O.J. Soto Sandoval[27,40], M. Spurio[4,5], N. Starkov[3], J. Steggemann[6], I. Timiryasov[35], V. Tioukov[1], F. Tramontano[1,2], C. Trippl[6], E. Ursov[3], A. Ustyuzhanin[1,37], G. Vankova-Kirilova[11], G. Vasquez[7], V. Verguilov[11], N. Viegas Guerreiro Leonardo[10], C. Vilela[10], C. Visone[1,2], R. Wanke[18], E. Yaman[23], Z. Yang[6], C. Yazici[23], C.S. Yoon[29], E. Zaffaroni[6], J. Zamora Saa[27,32]

[1]Sezione INFN di Napoli, Napoli, 80126, Italy
[2]Università di Napoli "Federico II", Napoli, 80126, Italy
[3]Affiliated with an institute covered by a cooperation agreement with CERN
[4]Sezione INFN di Bologna, Bologna, 40127, Italy
[5]Università di Bologna, Bologna, 40127, Italy
[6]Institute of Physics, EPFL, Lausanne, 1015, Switzerland
[7]Physik-Institut, UZH, Zürich, 8057, Switzerland
[8]Hamburg University, Hamburg, 22761, Germany
[9]European Organization for Nuclear Research (CERN), Geneva, 1211, Switzerland
[10]Laboratory of Instrumentation and Experimental Particle Physics (LIP), Lisbon, 1649-003, Portugal
[11]Faculty of Physics,Sofia University, Sofia, 1164, Bulgaria
[12]Università degli Studi di Cagliari, Cagliari, 09124, Italy
[13]University of Leiden, Leiden, 2300RA, The Netherlands
[14]Taras Shevchenko National University of Kyiv, Kyiv, 01033, Ukraine
[15]University College London, London, WC1E6BT, United Kingdom
[16]Università di Napoli Parthenope, Napoli, 80143, Italy
[17]Sungkyunkwan University, Suwon-si, 16419, Korea
[18]Institut für Physik and PRISMA Cluster of Excellence, Mainz, 55099, Germany
[19]Humboldt-Universität zu Berlin, Berlin, 12489, Germany
[20]Università del Sannio, Benevento, 82100, Italy
[21]Sezione INFN di Bari, Bari, 70126, Italy
[22]Università di Bari, Bari, 70126, Italy
[23]Middle East Technical University (METU), Ankara, 06800, Turkey
[24]Università della Basilicata, Potenza, 85100, Italy
[25]Departamento de Física, Pontificia Universidad Católica de Chile, Santiago, 4860, Chili
[26]Imperial College London, London, SW72AZ, United Kingdom
[27]Millennium Institute for Subatomic physics at high energy frontier-SAPHIR, Santiago, 7591538, Chile
[28]Ankara University, Ankara, 06100, Turkey
[29]Department of Physics Education and RINS, Gyeongsang National University, Jinju, 52828, Korea
[30]Gwangju National University of Education, Gwangju, 61204, Korea
[31]Nagoya University, Nagoya, 464-8602, Japan
[32]Center for Theoretical and Experimental Particle Physics, Facultad de Ciencias Exactas, Universidad Andrès Bello, Fernandez Concha 700, Santiago, Chile
[33]Korea University, Seoul, 02841, Korea
[34]Toho University, Chiba, 274-8510, Japan
[35]Niels Bohr Institute, Copenhagen, 2100, Denmark

[36]Present address: Faculty of Engineering, Kanagawa, 221-0802, Japan
[37]Constructor University, Bremen, 28759, Germany
[38]Chulalongkorn University, Bangkok, 10330, Thailand
[39]Chiang Mai University , Chiang Mai, 50200, Thailand
[40]Departamento de Física, Facultad de Ciencias, Universidad de La Serena, La Serena, 1200, Chile
[41]Also at: Università di Pisa, Pisa, 56126, Italy
[42]Currently at: Pakistan Institute of Nuclear Science and Technology (PINSTECH), Nilore, 45650, Islamabad Pakistan